PAPER

Symmetric charge exchange for intermediate velocity noble gas projectiles

IOP Publishing Journal of Physics B: Atomic, Molecular and Optical Physics
J. Phys. B: At. Mol. Opt. Phys. **52** (2019) 215203 (6pp) https://doi.org/10.1088/1361-6455/ab42d1

Symmetric charge exchange for intermediate velocity noble gas projectiles

Steven Bromley[1], **C E Sosolik** and **J P Marler**

Department of Physics and Astronomy, Clemson University, SC, United States of America

E-mail: sjbroml@clemson.edu, sosolik@clemson.edu and jmarler@clemson.edu

Received 23 May 2019, revised 30 August 2019
Accepted for publication 9 September 2019
Published 7 October 2019

Abstract

Experimental measurements of the total charge exchange cross section for 0.2–5.0 keV noble gas ions (He^+, Ne^+, Ar^+, Kr^+) with neutral atomic targets of the same species have been performed. The results are compared to theoretical predictions across this energy range as well as to prior data where available. Including these new results into the fitting parameters of state-of-the-art models brings prior measurements at higher energies into agreement. Merits of the two competing theories are discussed in the context of the four noble gas ions He^+ through Kr^+.

Supplementary material for this article is available online

Keywords: charge exchange, ion-atom collision, total cross section

1. Introduction

Charge transfer of an electron from a neutral atom to an ion is a fundamental interaction that plays a dominant role in the energy balance of atmospheric and astrophysical plasmas [1, 2]. In fusion experiments, the neutral-to-background plasma charge exchange can affect the particle and energy balance and can also serve as a useful monitor of that balance [3]. Here we explore the case of symmetric charge exchange, represented as

$$A^+ + A \rightarrow A + A^+, \tag{1}$$

where the ion and the neutral are the same species A. While this is a simple resonant process with no collision energy threshold, it has relevance in certain applied contexts, such as in the ionization balance of Hall Effect thrusters [4, 5].

In general, charge exchange cross sections, σ, are categorized by the collision energy or velocity, v, of the projectile ion. At intermediate velocities ($10^5\,\mathrm{cm\,s^{-1}} < v < 10^8\,\mathrm{cm\,s^{-1}}$), the velocity dependence is typically presented as

$$\sigma^{\frac{1}{2}}(v) = -k_1 \ln(v) + k_2, \tag{2}$$

where k_1 and k_2 are calculated from the ionization potential of the species A and from statistical considerations of the average impact parameter [6, 7]. The theoretical result (equation (2)) was first derived by Firsov [8] and independently by Dalgarno and McDowell [9] as highlighted by McDowell and Coleman [10]. Note in symmetric charge transfer, detailed balancing is also satisfied, see the work of Dalgarno and Yadav [11]. In short, the ion and neutral (A^+ and $A^+ + e^-$) are treated as a non-stationary state of the collision complex (A_2^+) with the dependence on the ionization potential arising from the symmetric and antisymmetric stationary states of that complex. The simplest case of the exchange, where only a single s-electron is considered, was treated by Rapp and Francis (RF) [6]. This was later expanded by Hodgkinson and Briggs (HB) to accommodate the exchange of electrons with values of higher angular momentum [7]. In the absence of non-resonant terms that may contribute at higher velocities, one can qualitatively interpret the v-dependence in equation (2) as a reflection of the interaction time available for the resonant event, i.e. higher v-values shorten the time for exchange and σ is decreased.

Calculated values of symmetric charge exchange cross sections for the noble gases have been available for some time [6]. With recent corrections, large discrepancies between these values and experimental data have been significantly reduced [7, 12]. While these corrected results are in particularly good agreement with intermediate velocity data obtained for Ar, significant differences remain and the corrected cross sections and experimental data can differ by up to 25% across the noble gas species. To address these discrepancies we have explored the intermediate velocity range, measuring the

[1] Author to whom any correspondence should be addressed.

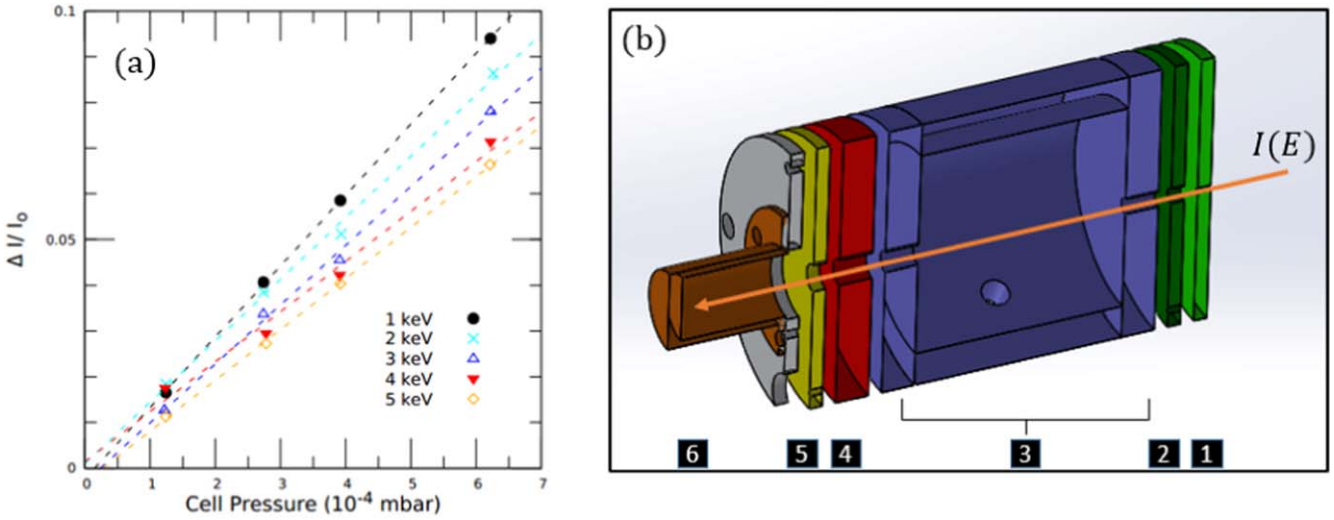

Figure 1. (a) Pressure-dependent current loss data obtained for the $Ar^+ + Ar$ charge exchange process at incident ion energies of 1–5 keV. (b) Schematic of the gas cell used for charge exchange measurements: 1. Faceplate, 2. Skimmer, 3. Gas cell, 4. Retarding field analyzer, 5. Suppression electrode, 6. Faraday cup.

symmetric charge exchange cross sections for He, Ne, Ar, and Kr species.

In the sections below, we discuss our experimental techniques (section 2) and present the results for these four species (section 3). These results are compared with several previous measurements and theoretical predictions (section 4).

2. Experiment

To measure the total, single charge exchange cross sections for noble gas species, beams of 0.2–5.0 keV A^+ ions (A = He, Ne, Ar, Kr) were generated in an OMICRON ISE 10 ion source from research grade gas at source pressures of 1–7 $\times$ 10^{-4} mbar. The generated ion beams were focused onto a gas cell apparatus located 370 mm from the ion source [13]. For these measurements, the gas cell was mounted on an UHV manipulator. The gas cell was aligned with the ion beam by maximizing the transmitted current through an empty (no injected gas) cell. A schematic of the gas cell apparatus is shown in figure 1 which also shows representative pressure-dependent transmission data with an Ar ion beam.

Ions enter the cell by passing through a faceplate (1 mm aperture, 2.5 mm thick), skimmer (2 mm aperture, 2.5 mm thick) and front end cap (3 mm aperture, 6.3 mm thick). They then pass through the gas cell body (40 mm length), back end cap (4 mm aperture, 6.3 mm thick), retarding field analyzer (5 mm aperture, 6.3 mm thick) and suppression electrode (6 mm aperture, 2.5 mm thick, held at −120 V) before being collected as ion current in a Faraday cup (FC). The dimensions of the cell and the aperture diameters were chosen to allow for the collection of all ions scattered within ±2.0° of the incoming beam at the front of the cell and ±13.0° at the back of the cell.

The pressure within the cell was measured using a full range Bayard-Alpert gauge connected by 350 mm of flexible stainless steel tubing. The pressure values obtained from this gauge were rescaled by a gas-dependent correction factor supplied by the manufacturer. Prior to the introduction of gas into the cell, the gas cell and vacuum chamber pressures were 3 $\times$ 10^{-7} mbar and 5 $\times$ 10^{-8} mbar respectively. During a typical measurement, the ratio of the gas cell-to-chamber pressure varied between 750 (for He) to 1000 (for Ar).

As in [13], the total charge exchange cross section in the single collision regime may be written using the measured values of the ion beam current collected in the FC with no gas in the cell (I_0) and that measured with gas in the cell for a beam with kinetic energy ϵ ($I(\epsilon)$) as

$$\sigma_{cx}(\epsilon) = \frac{k_b T}{PL}\left(\frac{I_0 - I(\epsilon)}{I_0}\right), \tag{3}$$

where k_b is the Boltzmann constant, T is the absolute temperature of the neutral gas (296 K), P is the pressure of the neutral gas in the gas cell, and L is the effective path length of the interaction region (52.6 mm). The linear pressure dependence for the attenuated beam currents for all the experimental measurements confirms that these data were obtained in the single collision regime ($P < 10^{-3}$ mbar). The initial current or I_0 values were recorded following a tuning of the ions through the empty cell. Gas was leaked into the cell and $I(\epsilon)$ was measured for at least four different cell pressures across the gas cell pressure range (1 − 8 $\times$ 10^{-4} mbar) at a given beam energy. The observed, fractional drop in ion beam current $\left(\frac{I_0 - I(\epsilon)}{I_0}\right)$ was then plotted as a function of the pressure and fit to obtain the cross section, σ_{cx}, using equation (3). The above procedure was repeated four times and the statistical uncertainty calculated from the standard deviation of the measurements at each energy are plotted for all of the data shown in section 3. Additionally, the systematic uncertainty

in the magnitude of the cross sections is estimated to be ± 17% [13].

The apparatus and procedure measure the total attenuation from the initial ion beam attributed to neutralization of ions in the beam by single charge exchange. However, other (non-CX) processes should be considered, i.e. ionization, elastic scatter, and inelastic scatter. While the cross sections for ionization of neutrals by ions in these specific systems are unmeasured, the values obtained for a comparable system are found to be approximately 10^{-18} cm^2 [14] or nearly three orders of magnitude below the σ_{cx} values obtained here. For the elastic and inelastic processes, differential cross section data for these species have been obtained by other groups (He [15, 16], Ne [17], Ar [17, 18], Kr [17]). In these data, the authors find that the cross section for elastic scatter is comparable to that of charge exchange. However, differential cross-section measurements show the data to be strongly peaked in the forward direction. Given the acceptance angle of our gas cell apertures, ions participating in forward peaked elastic scatter are not attenuated from the beam. In these noble gas reactions, inelastic scatter is preferentially through angles greater than several degrees but the magnitudes are small compared to the magnitude of elastic scattering cross sections at these energies.

A final consideration is the ion beam source in which ions are produced by electron bombardment which could lead to the production of excited ions. However, the velocity of the ions ($\approx 10^6$ cm s^{-1}) and the distance from the ion source to the gas cell ensure that all but metastable ions have decayed to the ground state before entering the gas cell. To check the effect of metastable ions in the incident beam on the measured cross sections, measurements were repeated at various ion source pressures, which should modulate the metastable population. No measurable effect was found. Therefore, it is assumed that the fraction of metastable ions present in the incident beam is small enough to be negligible.

Historically, symmetric cross sections were obtained by measuring ion beam current losses after passing through a gaseous target, and the charge exchange cross section is calculated in one of two ways. The cross section may be calculated from integrating a set of measured differential cross sections (e.g. [15]), or only the total cross section is obtained as in [19]. In literature involving the first case, the differential cross sections are measured with large step sizes between collision energies (∼keV). Additionally, these measurements are often complicated by small beam currents which are sensitive to fluctuations in ion source conditions. In the second case, misalignment of the ion beam and/or scattering outside of the acceptance angle of the detector can contribute to systematic errors. In the literature, most works have restricted themselves to 'low' ($E < 1$ keV) or 'high' ($E > 1$ keV) energies. In this work, the UHV manipulator allows for precise alignment with the center of the ion beam, and the large angular acceptance allows for collecting all collision products within the expected range of forward scatter. Combined with the energy range of our apparatus, 0.2–5.0 keV, our cross sections may be used to bridge the gaps between previous experiments and benchmark the available predictions across the intermediate regime.

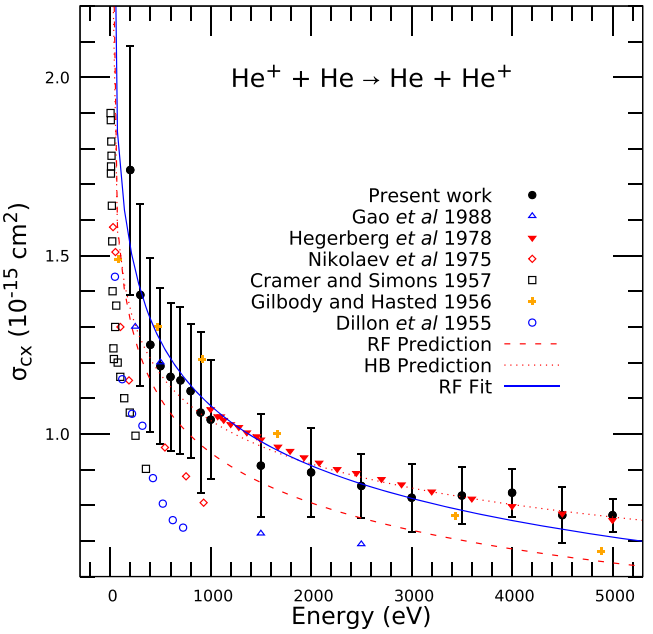

Figure 2. Current and prior [15, 19–22] measurements of the total charge exchange cross section for $He^+ + He$. The error bars shown represent statistical uncertainty in these measurements which also have a systematic uncertainty ±17%. Theoretical treatments based on equation (2) from Rapp and Francis (RF) [6] and Hodgkinson and Briggs (HB) [7] as well as a fit of the present measurements to equation (2) are shown as dashed red, dotted red, and solid blue lines respectively.

3. Results

Here we present the energy-dependent cross sections for symmetric charge exchange obtained for the noble gas species: He, Ne, Ar, and Kr. The data are compared with prior measurements for these systems as well as the predicted dependency which comes from equation (2) and the treatments of RF and HB.

The total charge exchange cross section obtained for He^+ on He between 0.2 and 5.0 keV is shown in figure 2 and on an expanded scale in figure 3. We observe the expected qualitative trend, which is a reduction in σ_{cx} as a function of the ion energy. In addition, our data show an overall agreement with multiple previous measurements on this system which serves to validate our experimental approach. There is a deviation from prior data below 1000 eV which can be attributed to the different methods used in those measurements (Gilbody and Hasted [20] and Nikolaev *et al* [21]) in particular to the assumptions made about the role of inelastic processes at higher pressures. Figures 2 and 3 also show the predicted energy-dependence based on the treatments of RF and HB. Both methods agree with the present intermediate velocity results, and the RF agreement extends out to include the higher energy results (figure 3) obtained by others.

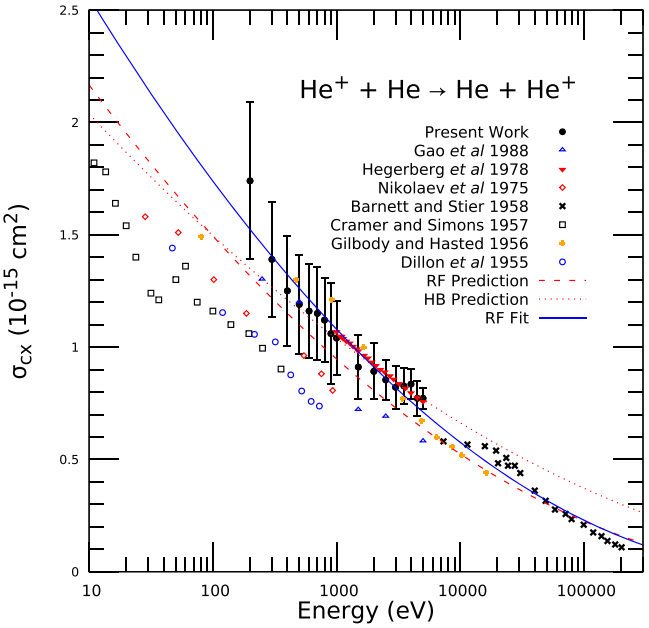

Figure 3. Total charge exchange cross section for $He^+ + He$ on an expanded energy scale. The error bars shown represent statistical uncertainty in these measurements which also have a systematic uncertainty ±17%.

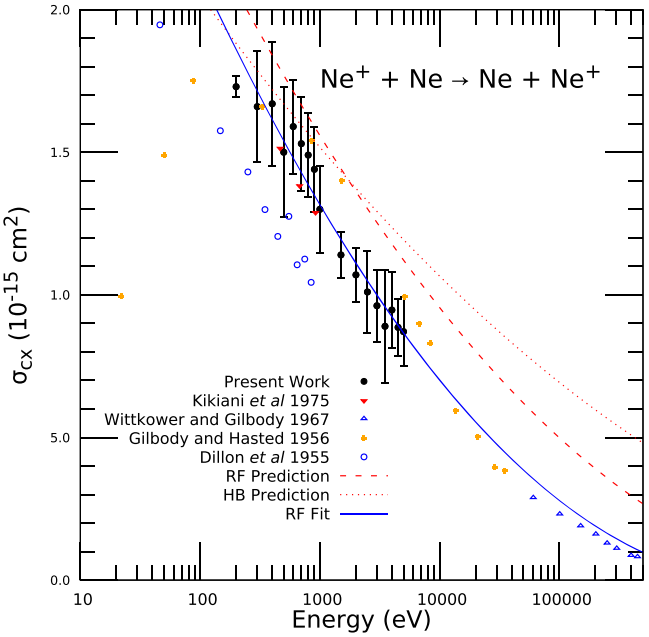

Figure 4. Total charge exchange cross section for $Ne^+ + Ne$ on an expanded energy scale. The error bars shown represent statistical uncertainty in these measurements which also have a systematic uncertainty ±17%.

Our results for Ne^+ charge exchange cross sections between 0.2 and 5.0 keV are shown in figure 4 as well as prior results obtained for this system that extend well out beyond 1 MeV [20, 23, 24]. The current data appear to be in good agreement with the measurements of Kikiani *et al* [23] and Gilbody [20] but differ significantly from those of Dillon *et al* [24]. Given the much different setup used in [24], especially with respect to a possible underestimation of the path length

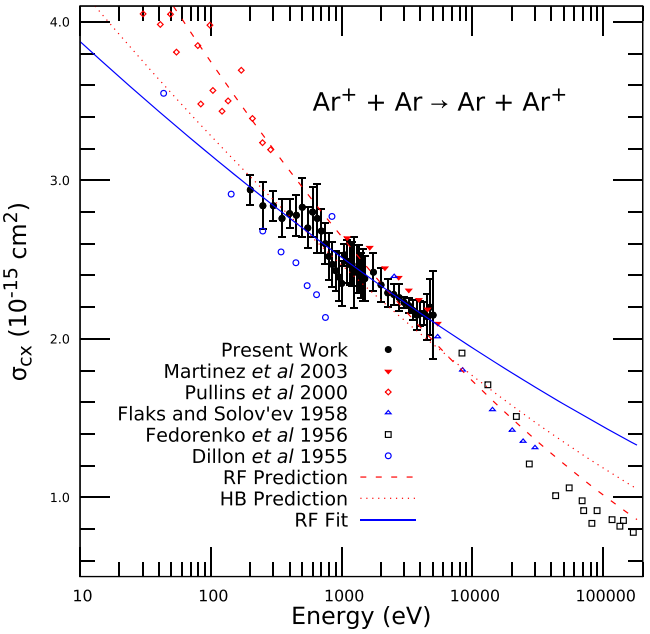

Figure 5. Total charge exchange cross section for $Ar^+ + Ar$ on an expanded energy scale. The error bars shown represent statistical uncertainty in these measurements which also have a systematic uncertainty ±17%.

over which the charge exchange has occurred, it is reasonable to assume the cross sections obtained by these authors are suppressed. As in the He case, also shown are the results from the treatments of RF and HB. Both the RF and HB results consistently overestimate the cross section above 1 keV compared to the present results.

Figure 5 shows the total charge exchange cross sections for Ar^+ on Ar as well as other prior measurements [12, 13, 24–26]. These include our own previous measurements obtained during the benchmarking of the apparatus [13]. For the intermediate velocity range we show excellent agreement with the measurements of Martinez *et al* [25] while the results of Dillon *et al* [24], as noted previously, appear suppressed compared to the current data. Both the RF and HB treatments appear to agree with our measured cross sections; however, significant deviations are apparent at both lower and higher energies for the HB result. Compared to the previous low energy results, the trend of our cross sections beneath 1keV is inconsistent with both the work of Pullins *et al* [12] and the RF prediction. While it is possible that our source produces both the metastable Ar^+ ($^2P_{1/2}$) and ground Ar^+ ($^2P_{3/2}$) ions, which differ in cross section by as much as 10% beneath 1 keV [12], the population of metastable Ar^+ ($^2P_{1/2}$) is expected to be small as discussed in section 2. The discrepancy between the present work and Pullins *et al* is unexplained.

Figure 6 shows the data obtained for the $Kr^+ + Kr$ cross section as well as other experimental measurements [5, 24, 27, 28]. The most contemporary data are from Hause *et al* [5] who measured cross sections in the range of 1–300 eV using the guided ion beam technique. Those results, which overlap with the current data at 300 eV, differ by only 4% at this point. Overall, below 1000 eV the current data are

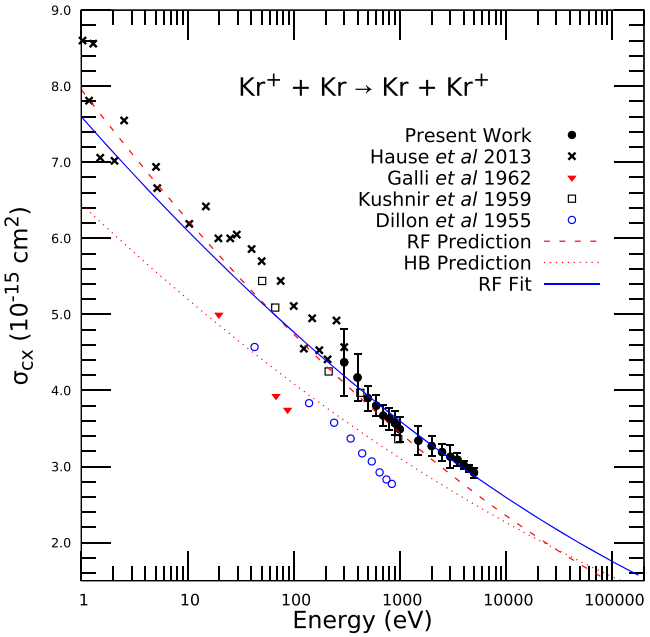

Figure 6. Total charge exchange cross section for $Kr^+ + Kr$ on an expanded energy scale. The error bars shown represent statistical uncertainty in these measurements which also have a systematic uncertainty $\pm 17\%$.

Table 1. Values of the two parameters k_1' and k_2' for theory [6, 7] and experimental fits. Values listed give cross sections in cm^2 with energy E in eV.

Element		k_1' ($\times 10^{-9}$)	k_2' ($\times 10^{-8}$)
He	HB prediction	2.808	5.161
	RF prediction	3.424	5.443
	RF fit	3.845	5.491
Ne	HB prediction	2.741	5.790
	RF prediction	3.722	6.520
	RF fit	4.251	6.565
Ar	HB prediction	3.309	7.253
	RF prediction	4.252	8.080
	RF fit	2.631	6.831
Kr	HB prediction	3.551	8.013
	RF prediction	4.415	8.919
	RF fit	3.822	7.724

in agreement with the work of Kushnir *et al* [28] but appear higher than the measurements of Galli *et al* [27] and, as in the other systems studied, the data of Dillon *et al* [24]. The RF prediction is in excellent agreement with the present work and Kushnir *et al* [28] below 1 keV. In this energy range, the HB prediction is smaller by as much as 7%. A fit of the present work to the RF functional form is similar to the RF Prediction at low energy and in agreement with the work of Hause *et al* [5]. In the extrapolation of the fit curve to energies above 5 keV, where experimental measurements do not exist for Kr, the fit curve and the RF prediction start to diverge. The good agreement of the extrapolated curve in He and Ne to the available experimental data is suggestive that the present measurements may be useful for determining the cross section at higher energies also. The numeric values of the fit parameters as well as those extracted from the published RF and HB predictions are recast in the form $\sigma_{cx}^{1/2}(E) = -k_1' \ln(E) + k_2'$ and listed in table 1.

4. Discussion

Total charge exchange cross sections for the symmetric reactions $A^+ + A \rightarrow A + A^+$ (A = He, Ne, Ar, Kr) in the energy range 0.2–5.0 keV are presented. All cross sections monotonically decrease as a function of energy and fit well to the expected functional form as expressed in equation (2). The RF and HB predictions are useful tools for predicting the magnitude of the charge exchange cross section in the measured energy range and require only knowledge of the ionization potential. However the agreement with the fit deviates at energies below 100's eV and greater than 10 keV as compared to previous measurements. At high energy, HB overestimates the magnitude for the He, Ne, and Ar. The RF prediction also overestimates the magnitude of the cross section in the case of Ne and Ar. (There is no experimental data for Kr in this energy range.) This is most likely due to the difficulty in including the contributions from different impact parameters correctly. As an alternative to relying solely on either theoretical calculation, fits of the functional form (equation (2)) to our current measurements better approximate the cross section at higher energies in the case of He and Ne as compared to the previous experimental data shown. The agreement in these two cases may not be so surprising as k_1 and k_2 are constant at high energies in the original derivation of equation (2).

However, at low velocities an average treatment of the impact parameter, which produces constant values for k_1 and k_2, may not be sufficient. At very low energies the charge exchange process is highly dependent on the electronic structure of the quasi-molecule formed through the course of the collision [6]. The representation of the wavefunction at low energies is complicated by the molecular states involved in the charge exchange process. To further develop a general expression for single charge exchange across an expanded energy range, full theoretical treatments of the A_2^+ (A = He, Ne, Ar, Kr) quasi-molecule and additional benchmarking experiments are required.

Acknowledgments

The authors gratefully acknowledge the work of the Physics and Astronomy Instrumentation Shop and financial support from the Clemson University College of Science.

ORCID iDs

Steven Bromley https://orcid.org/0000-0003-2110-8152
C E Sosolik https://orcid.org/0000-0001-6686-2584
J P Marler https://orcid.org/0000-0002-1626-5615

References

[1] Roble R G and Ridley C C 1987 *Ann. Geophys.* **5A** 369
[2] Larsson M, Geppert W D and Nyman G 2012 *Rep. Prog. Phys.* **75** 066901
[3] Kaita R *et al* 1986 *Nucl. Fusion* **26** 863
[4] Miller J S, Pullins H S, Levandier D J, Chiu Y and Dressler R A 2002 *J. Appl. Phys.* **91** 984
[5] Hause M, Prince B and Bemish R 2013 *J. Appl. Phys.* **113** 163301
[6] Rapp D and Francis D E 1962 *J. Chem Phys.* **37** 2631
[7] Hodgkinson D P and Briggs J S 1976 *J. Phys. B: At. Mol. Phys.* **9** 255
[8] Firsov O B 1951 *Zh. Eksp. Teor. Fiz.* **21** 1001–8
[9] Dalgarno A and McDowell M R C 1956 *Proc. Phys. Soc.* A **69** 615
[10] McDowell M and Coleman J 1970 *Introduction to the Theory of Ion-Atom Collisions* (Amsterdam: North-Holland)
[11] Dalgarno A and Yadav H N 1953 *Proc. Phys. Soc.* A **66** 173
[12] Pullins S H, Dressler R A, Torrents R and Gerlich D 2000 *Z. Phys. Chem.* **214** 1279
[13] Bromley S J, Fox D C, Sosolik C E, Harriss J E and Marler J P 2018 *Rev. Sci. Instrum.* **89** 073107
[14] Shah M B, Geddes J, McLaughlin B M and Gilbody H B 1998 *J. Phys. B: At. Mol. Opt. Phys.* **31** L757
[15] Gao R S, Johnson L K, Schafer D A, Newman J H, Smith K A and Stebbings R F 1988 *Phys. Rev.* A **38** 2789
[16] Baudon J, Barat M and Abignoli M 1968 *J. Phys. B: At. Mol. Phys.* **1** 1083
[17] Barat M, Baudon J, Abignoli M and Houver J C 1970 *J. Phys. B: At. Mol. Phys.* **3** 230
[18] Sidis V, Barat M and Dhuicq D 1975 *J. Phys. B: At. Mol. Phys.* **8** 474
[19] Hegerberg R, Stefansson T and Elford M T 1978 *J. Phys. B: At. Mol. Phys.* **11** 133
[20] Gilbody H B and Hasted J B 1957 *Proc. R. Soc.* **238** 334
[21] Nikolaev V S, Dmitriev I S, Fateeva L N and Teplova Y A 1975 *Sov. Phys. JETP* **40** 23
[22] Cramer W H and Simons J H 1957 *J. Chem. Phys.* **26** 1272
[23] Kikiani B I, Saliya Z E and Bagdasarova I G 1975 *Zh. Tekh. Fiz.* **45** 586
[24] Dillon J A, Sheridan W F, Edwards H D and Ghosh S N 1955 *J. Chem. Phys.* **23** 776
[25] Martinez H, Castillo F, Reyes P and Santibañez F 2003 *Int. J. Mass Spectrom.* **228** 107
[26] Flaks L P and Solov'ev E S 1958 *Sov. Phys. Tech. Phys.* **3** 564
[27] Galli A, Giardini-Guidoni A and Volpi G G 1962 *Il Nuovo Cimento (1955-1965)* **26** 845
[28] Kushnir R M, Palyukh B M and Sena L A 1959 *Izv. Akad. Nauk SSSR Ser. Fiz.* **23** 1007